UDC 621.3 https://doi.org/10.20998/2074-272X.2025.5.02

H. Hafaiedh, Y. Saoudi, A. Benamor, L. Chrifi-Alaoui

Wind farms integration into power system with improved location and stability problem solving

Problem. *This article investigates as a consistent supply to satisfy rising world energy consumption, wind energy is becoming more and more important. Correct evaluation of the stability and performance of wind induction generators inside power systems remains difficult, particularly in regard to ensuring compliance with grid rules and best location.* ***Goal.*** *To evaluate and compare the dynamic behavior and grid compatibility of the squirrel cage induction generator (SCIG) and the doubly fed induction generator (DFIG) wind generators in various locations within the IEEE 14 bus network, and to determine the improved generator type and location.* ***Methodology****. The investigation adopts the small signal stability analysis for modeling the wind induction turbines due to its capability to assess system stability, controllability and observability. The IEEE 14 bus distribution network is modeled with wind generators interconnected at buses 10 through 14. Several parameters are analyzed under different operating conditions, including voltage, rotor angle, active power, reactive power and frequency.* ***Results.*** *DFIG exhibits superior performance across all analyzed parameters, particularly in maintaining grid stability and meeting grid code requirements. Bus 13 was identified as the improved integration point for wind farms using DFIG technology.* ***Scientific novelty****. The study offers a structured comparison of SCIG and DFIG using state space modeling rarely applied in a direct bus by bus comparative study within a standard distribution network.* ***Practical value.*** *The results help system planners choose the right wind turbine type and location, which promotes a more reliable and effective integration of renewable energy sources into power networks.* References 51, tables 5, figures 7.

Key words: **squirrel cage induction generator, doubly fed induction generator, best location of wind farms, IEEE 14 bus network.**

Проблема*. У статті розглядається вітряна енергія як джерело безперебійного живлення для задоволення світового споживання енергії, що зростає, і її роль у цьому процесі. Коректна оцінка стабільності та продуктивності вітрогенераторів в енергосистемах залишається складним завданням, особливо з точки зору забезпечення відповідності вимогам електромережі та вибору оптимального розташування.* ***Мета****. Оцінка та порівняння динамічної поведінки і мережевої сумісності вітрогенераторів з короткозамкненим ротором (SCIG) та асинхронним генератором з подвійним живленням (DFIG) у різних місцях мережі IEEE 14, а також визначення покращеного типу та міста розташування генератора.* ***Методологія****. У дослідженні для моделювання вітрогенераторів використовується аналіз стійкості при малих сигналах завдяки його здатності оцінювати стійкість, керованість та спостережливість системи. Розподільна мережа IEEE 14 моделюється з вітрогенераторами, з'єднаними між собою на шинах 10-14. Аналізуються різні параметри за різних робочих умов, включаючи напругу, кут ротора, активну потужність, реактивну потужність та частоту.* ***Результати****. DFIG демонструє кращі характеристики за всіма проаналізованими параметрами, особливо щодо підтримки стабільності мережі та відповідності вимогам мережевого кодексу. Шина 13 була визначена як покращена точка інтеграції для вітропарків, які використовують DFIG.* ***Наукова новизна****. Дослідження пропонує структуроване порівняння SCIG та DFIG з використанням моделювання простору станів, що рідко застосовується при прямому порівняльному дослідженні шин у стандартній розподільній мережі.* ***Практична значимість****. Результати допомагають системним планувальникам вибрати правильний тип та місцезнаходження вітрогенератора, що сприяє більш надійній та ефективній інтеграції відновлюваних джерел енергії в енергомережі.* Бібл. 51, табл. 5, рис. 7.

Ключові слова: **асинхронний генератор з короткозамкненим ротором, асинхронний генератор з подвійним живленням, найкраще розташування вітряних станцій, шина живлення IEEE 14.**

Introduction. Wind energy is seen as an endless supply of clean energy as compared to other energy sources like nuclear, coal, gas and oil. When it was adopted, the use of fossil fuels greatly decreased. Globally, wind power plant construction has increased dramatically during the last twenty years [1–4].

Globally, installed wind energy capacity exceeded 100 GW by the end of 2023, as stated by the Global Wind Energy Council [5]. This is a 15 % increase globally over 2022 in installed capacity [6]. It's also the year with the most wind energy of all time. As of 2022, there were 906 GW of installed capacity for wind energy globally, a 9 % growth. One major problem for wind energy is the constant variations in temperature, density, and wind speed. To prevent unfavorable effects on grid electricity, the integration of wind turbines into the grid must be supervised by specific laws or grid codes [1, 7–9]. The operational restrictions and environmental variables of different countries influence the grid codes produced [10, 11]. Like a traditional power plant, wind farms need a connection to the grid that minimizes interruptions.

In wind turbines, 3 different kinds of power generation devices are typically utilized to transform electrical energy from wind: doubly fed induction generator (DFIG), permanent magnet synchronous generator (PMSG), squirrel cage induction generator (SCIG). Among these generators, DFIG has stayed connected to the power system and has demonstrated good performance in low voltage ride through incidents [12]. Because of their significant advantages, such as increased energy efficiency, improved power quality, ease of control and variable speed handling, DFIGs are frequently utilized in systems that convert wind energy [13]. However, due to their robustness, affordability and ease of use [14], wind power conversion systems equipped with SCIGs also use reactive power compensators.

Consequently, precise modeling of induction generator is needed for research utilizing computer simulations, investigations, and research in order to effectively handle their major issues, especially with relation to the grid installation of wind energy conversion technologies. Understanding the utilization of wind power and how it integrates with the grid has thus become crucial research [15].

It is vital to do in depth research to comprehend how wind farms and the power grid interact. A wind farm in the design phase involves a number of research projects, which are carried out in a manner akin to that of other new technological facilities [13, 15]. Model planning, which takes into account variables like voltage, electricity flow, reactive power capability, short-circuit currents and the transient stability, is typically used to assess the effects of wind technology [16–19]. It is common practice to take into account a thorough depiction of every single unit as well as the relationships between units and the system.

As an alternative, when considering the wind farm from the standpoint of the system, it can be treated as a lumped equivalent model [17]. Additional related research focuses on improving transient stability and dispatching spinning reserves in wind-thermal power systems [20, 21].

The authors of [22] examined the differences in performance between wind turbines connected to the power system that were induction generators, DFIG and PMSG. By taking into account a 3-phase defect at the end of a transmission line, the machines efficiency are assessed. Using MATLAB software, the performance of grid connected 5-phase modular PMSG with various slot and pole number combinations is assessed in [23].

Additionally, the technological difficulties of integrating wind were covered in earlier studies [24] energy into the grid. The primary obstacles to wind energy grid integration are discussed in [4], including the consequences of power quality, power imbalances, wind power on the power system and operating costs. The comparison of the grid integration impact of DFIG and SCIG is examined in [25]. This research [26] compares the performance of SCIG and DFIG wind turbines under various conditions through MATLAB/Simulink. The results indicate that DFIG is more efficient, especially in variable speed generation and power regulation, making it more compatible with large wind farms connected to weak grids.

The **goal** of this work is to evaluate and compare the dynamic behavior and grid compatibility of SCIG and DFIG wind generators in various locations within the IEEE 14 bus network, and to determine the improved generator type and location. The working conditions for producing reactive and active power, as well as voltage, angle theta, industrial frequency, and stability, were the primary subjects of the analysis. Numerous simulation programs have been examined for the analysis and modeling of wind farms, as well as for improved location and stability problem solving. The Power System Analysis Toolbox (PSAT) was selected because it offered sophisticated simulation tools and could be used for the necessary analysis.

1. Modeling of wind energy. The wind turbines capture wind energy through their blades and convert it into mechanical power. This process is influenced by various factors such as wind speed, blade design, and the area swept by the blades. To assess the efficiency of energy conversion, specific mathematical models that incorporate these elements can be applied. By optimizing turbine performance, wind energy can be effectively harnessed and used for power generation. Through the turbine blades, wind energy is converted to power, which is given as follows:

$$P_{wi} = T_{me} \cdot \omega_m; \tag{1}$$

$$T_{me} = P_{wi} / \omega_m, \tag{2}$$

where P_{wi}, T_{me} are the generated power and mechanical torque respectively; ω_m is the rotor angular speed.

The power generated by the wind is expressed as follows [27–30]:

$$P_{wi} = 0.5\zeta_p(\lambda, \beta)\rho\pi R^2 V^3, \tag{3}$$

where ζ_p is the power coefficient; λ, β are the blade pitch angle and the tip speed ratio respectively; ρ is the air density; R is the radius of the turbine blades; V is the wind speed.

The tip speed ratio λ is determined as:

$$\lambda = \omega_m R / V. \tag{4}$$

The rotor angular speed ω_m is:

$$\omega_m = 2\pi n / 60, \tag{5}$$

where n is the rotational speed.

The power coefficient ζ_p is [5]:

$$\zeta_p = 0.44\left(\frac{125}{\lambda_j} - 6.94\right)e^{16.5/\lambda_j}, \tag{6}$$

where λ_j is the tip speed ratio coefficient at the j^{th} element of the turbine blade:

$$\lambda_j = \frac{1}{1/\lambda + 0.002}. \tag{7}$$

2. Configuration induction generator. Wind turbines can be classified into different types, with 2 common ones using induction generators. These turbines use induction generators to convert wind energy into electrical power. In an induction generator, the rotor is driven by the wind, creating a rotating magnetic field that induces electrical current in the stator. The key advantage of these turbines is their simplicity and cost effectiveness, as they can operate asynchronously with the grid. They are reliable and require minimal maintenance, making them suitable for various wind conditions and widely used in both small and large scale energy projects. In this section, the configurations of these turbines will be explored, detailing their design and operation. Additionally, the mathematical models associated with each type will be presented. A comparison will then be made, evaluating their performance, power quality, and reliability.

2.1. Modeling of induction generator. Induction generators are commonly used in wind energy systems due to their simplicity and reliability. These generators convert mechanical energy from the turbine into electrical power through electromagnetic induction. Modeling an induction generator involves understanding key parameters like rotor and stator voltages, which directly impact performance and efficiency. The mathematical formulas for modeling an induction generator by the rotor and stator voltage in *d-q* (direct and quadrature) axis [17–19] are:

$$\begin{cases} v_{dr} = R_r i_{dr} + \dfrac{\mathrm{d}\phi_{dr}}{\mathrm{d}t} + \omega_s \phi_{qr}; \\ v_{qr} = R_r i_{dr} + \dfrac{\mathrm{d}\phi_{dr}}{\mathrm{d}t} - \omega_s \phi_{qr}; \\ v_{ds} = R_r i_{ds} + \dfrac{\mathrm{d}\phi_{ds}}{\mathrm{d}t} + \omega_s \phi_{qs}; \\ v_{qs} = R_r i_{qs} + \dfrac{\mathrm{d}\phi_{ds}}{\mathrm{d}t} - \omega_s \phi_{ds}, \end{cases} \tag{8}$$

where v_{dr}, v_{ds}, v_{qr}, v_{qs} are the rotor and stator voltages respectively; i_{dr}, i_{qr} are the current of the rotor; i_{ds}, i_{qs} are the current of the stator; ϕ_{dr}, ϕ_{qr} are the flux of the rotor; ϕ_{ds}, ϕ_{qs} are the flux of the stator; v_s, v_r are the voltage of stator and rotor respectively.

The equations below present the flux linkage and electromagnetic torque:

$$\begin{cases} \phi_{dr} = L_m i_{ds} + L_{ro} i_{dr}; \\ \phi_{qr} = L_m i_{qs} + L_{ro} i_{qr}; \\ \phi_{ds} = L_m i_{dr} + L_{so} i_{ds}; \\ \phi_{qs} = L_m i_{qr} + L_{so} i_{qs}, \end{cases} \tag{9}$$

$$T_{el} = \phi_{qr}\, i_{dr} - \phi_{dr}\, i_{qr}, \tag{10}$$

where L_m is the mutual inductance; L_{so}, L_{ro} are the stator and rotor leakage inductance respectively; T_{el} is the electrical torque.

The mechanical equations are as follows:

$$\begin{cases} T_{el} = -\frac{3}{2} P_{wi} \frac{L_m}{L_{so}} \left(\phi_{ds} i_{qr} - \phi_{qs} i_{ds} \right), \\ \frac{\mathrm{d}\Omega_{me}}{\mathrm{d}t} = \frac{1}{J} \left(T_{me} - T_{el} - f \cdot \Omega_{me} \right), \end{cases} \quad (11)$$

where Ω_{me} is the angular acceleration; $\mathrm{d}\Omega_{me}$ is the angular velocity; f is the setting in the system; J is the inertia moment of the rotor.

These equations are used to limit how powers variation affects voltage amplitude and frequency [31–33]:

$$P = P_0 \left(1 + D_p \frac{f - f_n}{f_n} \right) \cdot \left(\frac{V}{V_0} \right)^{\alpha} \quad (12)$$

where P is the active power; P_0 is the reference active power; D_p is the active power sensitivity factor; V_0 is the voltage amplitude; α may indicate a load model parameter, potentially connected to the active power and another parameter, possibly related to the load dependency on voltage or frequency respectively.

Table 1 shows the different values of the constants for each load category. These load category parameters vary depending on the network. The coefficient D_p is used to illustrate the frequency bearing evolution of each electrical bus. Therefore, it is essential to introduce (12) to show the development of a significant dynamic grid element. In reality, there is a close connection between these variables and the installed loads.

Table 1

Parameters of the different load category

Load category	α	D_p
Winter	1.02	1.000
Summer	1.20	0.999
Industrial	0.80	1.000

2.2. The squirrel cage induction generator. The SCIG running at a steady pace is used in wind energy turbines that are directly linked to the grid [34, 35]. The generator is connected directly to the grid, much like in other wind energy conversion systems, while the turbine is associated with the SCIG through a gearbox to reach the necessary speed for power generation (Fig. 1). Since rotor slip is the primary cause of speed variations, variations in rotor speed are minimal, wind turbines usually run at a set speed. The SCIG absorbs reactive power by acting as an induction motor during changes in grid voltage. Pitch angle control is used to adjust generator rotor speed instabilities when wind speeds change, maximizing wind power output. Wind energy systems with varying speeds also use squirrel cage technology [36–42]. The SCIG data are presented in Table 2.

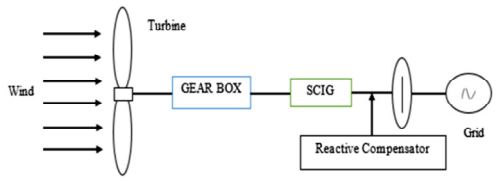

Fig. 1. The classic method of integrating SCIGs with the grid

Table 2

Wind turbine data for SCIG

Parameters	Value	Parameters	Value
Rated power, MVA	10	Stator reactance, p.u.	0.01
Rated voltage, kV	13.8	Rotor reactance, p.u.	0.08
Rated frequency, Hz	50	Mutual reactance, p.u.	3
Stator resistance, p.u.	0.01	Inertia constants [kW/kVA, kW/kVA, p.u.]	2.5, 0.5, 0.3
Rotor resistance, p.u.	0.1	Number of poles pairs	4

2.3. The double fed induction generator. Figure 2 shows the integrating DFIGs into the grid.

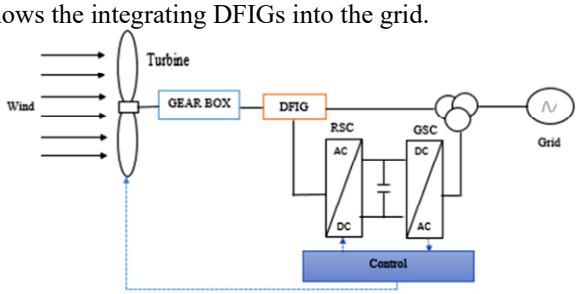

Fig. 2. Traditional integration of a DFIG with the grid

The rotor of the DFIG is associated with the wind turbines low speed shaft by a gearbox, which increases the speed to the necessary level so that the generator can generates electricity [34]. With 2 voltages source converters placed back-to-back and using a wound type rotor, the DFIG configures a grid-connected AC-DC-AC [41–46]. Normally, each converter runs at 30 % of the specified rated power of the generator. The converter connected to the rotor is known as rotor side converter (RSC), while the converter connected to the grid is known as grid side converter (GSC). These converters handle varying wind speeds well, making sure that the output frequency remains constant and in line with grid needs. They are divided using a DC capacitor in the intermediate circuit that works as an energy stock management device [16]. The step up transformer is a device that connects the stator to the network [13]. An integrated control system at the wind turbine shaft manages precise power, reactive power and voltage across the network. Different voltage commands are generated by this system for the RSC and GSC. The RSC ensures control of active and reactive powers, and the GSC ensures their operation at a unity power factor. The GSC also controls the voltage at the DC link capacitor between the RSC and the GSC. Table 3 shows the wind turbine data for DFIG used in the model.

Table 3

Wind turbine data for DFIG

Parameters	Value	Parameters	Value
Rated power, MVA	10	Mutual reactance, p.u.	3
Rated voltage, kV	13.8	Inertia constants, kW/kVA	3
Rated frequency, Hz	50	Pitch control gain, p.u.	10
Stator resistance, p.u.	0.01	Time constant, s	3
Rotor resistance, p.u.	0.1	Voltage control gain, p.u.	10
Stator reactance, p.u.	0.01	Power control gain, s	0.01
Rotor reactance, p.u.	0.08	Number of poles pairs	4

3. Small signal stability analysis is a crucial aspect of power system dynamics, used to assess the stability of the system when subjected to small disturbances. It helps to understand how the system responds to minor fluctuations and ensures that the system remains stable under normal operating conditions. The eigenvalue method can be used to analyze the small signal stability. This method is essential for identifying potential instabilities and improving system performance.

This approach works with linear models via examining where the poles are located inside the complex plane. The characteristic polynomial described by the following equation has poles as its solutions [47]:

$$det(\boldsymbol{A} - \lambda \boldsymbol{I}) = 0, \quad (13)$$

where *det* is the determinant of the matrix $(\boldsymbol{A} - \lambda \boldsymbol{I})$; $\boldsymbol{A}$ is the state matrix; $\boldsymbol{I}$ is the identity matrix of the same size as $\boldsymbol{A}$; λ is the eigenvalue.

In the latter, there is an imaginary portion and a real part. The real portion determines the analyzed system's convergence, whereas the oscillating behavior is correlated with the imaginary part. If every pole is in the complex plane's negative real portion, the system is considered stable.

The system model or its parameters determine the values of the poles. One may verify the model's stability domain by examining how the positions of the poles change with respect to the parameter values.

4. Results and discussion. In this section devoted to the results of the experiment and its analysis, one examines 3 key elements. First, one examines the performance of 2 types of generators employed in wind power systems: the SCIG and the DFIG. The disparities in stability, efficiency, and resistance to disruption between these 2 technologies are highlighted by this comparison. Subsequently, one examines the stability of the electricity network when integrating these generators. The basis of this analysis is the eigenvalue analysis of the system, which allows determining the conditions under which the network remains stable or can become unstable. Finally, one compares the results with those of other studies in order to evaluate the relevance of the findings and to place the study within the broader framework of existing research. The analysis highlights the methodological disparities and the obtained results, which allows having a more exhaustive vision of the consequences of integrating these generators into the electricity network.

4.1. Evaluation of 2 different types of generators. This section compares 2 types of wind power systems, including their performance and the market share each type currently enjoys. The influence of wind generation on the transient stability of the system is examined for wind farms using an aggregated model [48]. PSAT is utilized in this work to perform the transient stability analysis [49, 50]. There are 16 lines, 14 buses, 5 generators, 4 transformers and 11 loads in this system. The standard IEEE 14 bus data format has been used to load the buses and lines [48].

The following figures show several graphs comparing the performance of 2 types of wind turbine generators: the SCIG and the DFIG. Each graph shows different electrical parameters as a function of time for buses 10–14 of the network. Figure 3 presents the variation of the voltage profile for 2 types of wind turbines. It shows that the rotor inductance of DFIG is higher, which results in less variation in the magnetic field. Therefore, the voltage fluctuations are reduced, which decreases the voltage ripple compared to the other case and makes the voltage smoother.

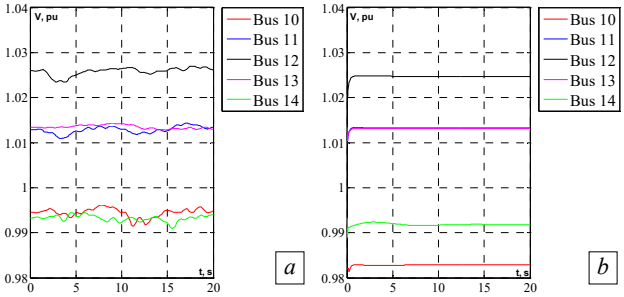

Fig. 3. The voltage for 2 different type of wind turbine: *a* – for SCIG; *b* – for DFIG

The following figure shows the variation of angle θ for the 2 types of wind turbines. The phase angle curves in Fig. 4 show that the phase angle ripples in DFIG are more stable and converge to a constant value. This is explained by the higher inertia compared to SCIG, which favors a better network synchronization with this type of generators.

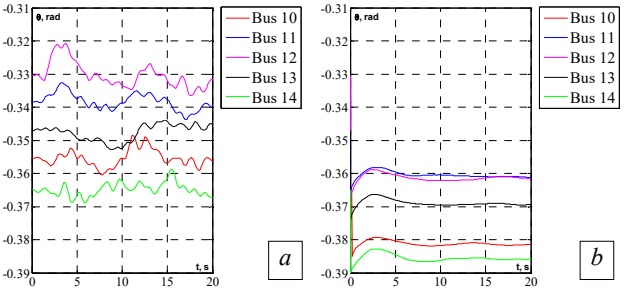

Fig. 4. The angle for 2 different type of wind turbine: *a* – for SCIG; *b* – for DFIG

Figures 5, 6 depict the variation of active and reactive power respectively over time for the 2 types of wind turbines. From the presented Fig. 5, the active power of the DFIG is more stable, with only slight fluctuations, indicating its better ability to provide constant active power. On the other hand, for the SCIG, oscillations are recorded on all critical buses, with less significant variations at bus 14.

For both types of wind turbines, Fig. 6 shows that the same reactive power is consumed to create the internal magnetic field. This reactive power is essential for the proper functioning of the generators, allowing them to produce the active power.

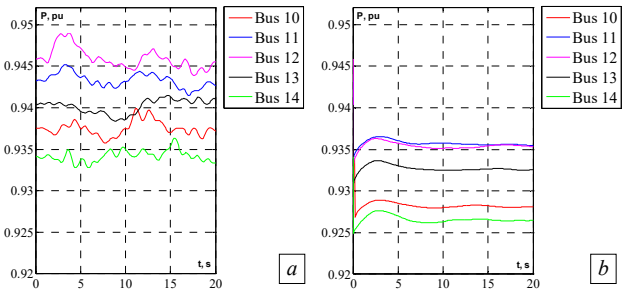

Fig. 5. The active power for 2 different type of wind turbine: *a* – for SCIG; *b* – for DFIG

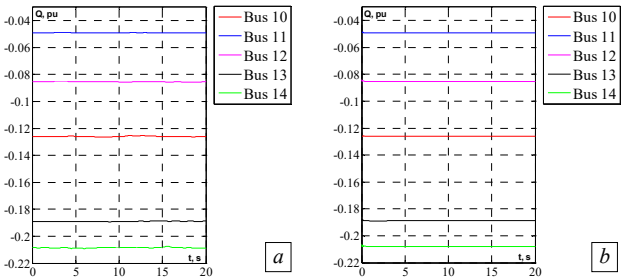

Fig. 6. The reactive power for 2 different type of wind turbine: *a* – for SCIG; *b* – for DFIG

Figure 7 shows the variation of frequency versus time for both types of SCIG and DFIG wind turbines under 3 conditions, represented by (12). This study examines the effect of wind turbine integration on frequency stability.

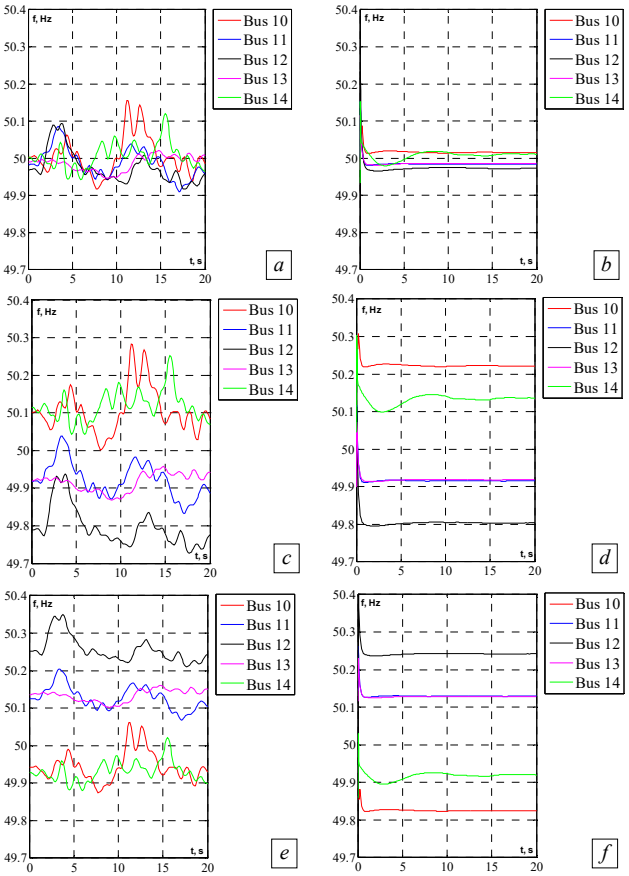

Fig. 7. Frequency performance analysis graphs of 2 types of wind turbines under different grid conditions: *a* – SCIG under winter conditions; *b* – DFIG under winter conditions; *c* – SCIG under summer conditions; *d* – DFIG under summer conditions; *e* – SCIG under industrial conditions; *f* – DFIG under industrial condition

According to Fig. 7, the system is strongly influenced by both grid and climatic conditions. It is affected by climatic variations, particularly in winter and summer, as well as by industrial factors and the type of equipment installed on the grid.

The grid integrated wind turbine is a DFIG type, which contributes to greater grid stability. Indeed, this figure generally illustrates frequency variation, which is influenced by the inertia of the DFIG. Since the inertia of the DFIG is higher than that of the SCIG, disturbances are more difficult to induce. Consequently, the DFIG provides greater grid stability. Furthermore, it is possible to produce approximately 2/3 of the power via the stator, while approximately 1/3 of the power can be recovered by the rotor thanks to the addition of a power electronics stage. This configuration allows power to be distributed between the rotor and stator, while minimizing overload on the stator windings.

4.2. Examination of the stability of the electrical network. Tables 4, 5 show the eigenvalue evaluation curves for 2 types of generators: the SCIG and the DFIG, in an electrical network, for buses 10–14. Table 4 shows that our network is more stable when DFIG is installed, because in case of SCIG, the minimum value of the eigenvalues is –0.25 p.u, while for DFIG it is –1 p.u. Thus, SCIG is very sensitive to instability, which can cause disturbances in the system and it causes a blackout phenomenon. In conclusion, bus 13 appears to be the most suitable location for wind turbine integration particularly with DFIG and SCIG technologies due to its ability to maintain voltage levels, phase angle, power flow, and frequency stability, thereby enhancing the overall stability of the network.

Table 4

Network eigenvalues with integration of a wind turbine to the buses

Bus	Eigenvalues of network with SCIG	Eigenvalues of network with DFIG
10	–7.5427+35.4824j –7.5427–35.4824j –10.1091+0j –0.89032+4.1965j –0.89032–4.1965j –0.25+0j	–100.9781+0j –0.6524+0j –0.25+0j –0.33333+0j –1+0j
11	–7.5704+35.2617j –7.5704–35.2617j –9.8834+0j –0.91571+4.2364j –0.91571–4.2364j –0.25+0j	–100.9315+0j –6.2085+0j –0.64742+0j –0.33333+0j –1+0j
12	–7.5704+35.2617j –7.5704–35.2617j –9.8834+0j –0.91571+4.2364j –0.91571–4.2364j –0.25+0j	–100.9315+0j –6.2085+0j –0.64742+0j –0.33333+0j –1+0j
13	–7.5178+35.3704j –7.5178–35.3704j –10.3942+0j –0.89366+4.2294j –0.89366–4.2294j –0.25+0j	–100.8581+0j –5.7772+0j –0.64476 +0j –0.33333+0j –1+0j
14	–7.4181+34.68222j –7.4181–34.68222j –9.3169+0j –0.92836+4.2348j –0.92836–4.2348j –0.25+0j	–101.282+0j –0.64034+0j –0.25+0j –0.33333+0j –1+0j

4.3. Comparative study. Table 5 contrasts the advised approaches with the current state of the art approaches. One has extended the approach from [51], which just uses an IEEE 14 bus network for voltage analysis. However, this approach is flawed since it fails to account for network frequency. One tested both voltage and frequency during the investigation because they are complementary.

Table 5

Comparison with the existing state of art methods

Bus number	Work [51]		Proposed work	
	V, p.u.	θ, rad	V, p.u.	θ, rad
1	1.06200	0.00000	1.06000	0.00000
2	1.04500	–0.13560	1.04500	–0.13451
3	1.01300	–0.33210	1.01000	–0.32979
4	0.99700	–0.26440	0.99800	–0.26152
5	1.00200	–0.22690	1.00300	–0.22553
6	1.07400	–0.36950	1.07000	–0.37431
7	1.03600	–0.33930	1.03700	–0.35054
8	1.09300	–0.33930	1.09000	–0.35054
9	1.01200	–0.37900	1.01600	–0.39755
10	1.01200	–0.38440	1.01500	–0.40046
11	1.03500	–0.37980	1.03600	–0.39025
12	1.04600	–0.90590	1.04800	–0.39615
13	1.03600	–0.39140	1.04000	–0.39863
14	0.99600	–0.41050	1.01300	–0.42544

In contrast to work [51], in which were used automatic voltage regulators (AVRs) and turbine

governors (TGs) in the network IEEE 14 bus, only TGs are used, which enables one to drastically cut costs. In contrast to [51], which compares the power factor (PF) on a single bus 14 when a wind turbine is integrated into the IEEE 14 network versus not, this work first compares the integration of 2 different kinds of wind turbines before calculating the PF on multiple buses (10–14) to identify the best wind turbine and where to put it.

Conclusions. Concretely, the integration of renewable energies is essential today in the face of the continuous increase in electricity consumption. Renewable energies, such as wind power, are inexhaustible, sustainable, and profitable. However, their production is highly dependent on natural conditions, making grid stability more difficult to ensure without appropriate monitoring mechanisms.

In this study, we modeled the integration of SCIG and DFIG generators into the IEEE 14 standard bus network using the small signal stability analysis approach to analyze their dynamic behavior and grid compatibility. The results show that DFIG offers better performance in terms of stability, voltage, frequency, and compliance with grid requirements. Bus 13 was identified as the optimal location for connecting a DFIG based wind farm.

Thus, the objective of this research, which was to evaluate and compare the dynamic performance of SCIG and DFIG generators and to determine their improved placement within the IEEE 14 bus network, was fully achieved.

Future research will focus on improving existing wind turbine technologies and jointly optimizing the placement of wind turbines and FACTS devices to improve the overall performance of the power grid.

Conflict of interest. The authors declare that they have no conflicts of interest.

REFERENCES

1. Giefer L.A., Staar B., Freitag M. FPGA–Based Optical Surface Inspection of Wind Turbine Rotor Blades Using Quantized Neural Networks. *Electronics*, 2020, vol. 9, no. 11, art. no. 1824. doi: https://doi.org/10.3390/electronics9111824.

2. Villena–Ruiz R., Honrubia–Escribano A., Jiménez–Buendía F., Molina–García Á., Gómez–Lázaro E. Requirements for Validation of Dynamic Wind Turbine Models: An International Grid Code Review. *Electronics*, 2020, vol. 9, no. 10, art. no. 1707. doi: https://doi.org/10.3390/electronics9101707.

3. Sahragard A., Falaghi H., Farhadi M., Mosavi A., Estebsari A. Generation Expansion Planning in the Presence of Wind Power Plants Using a Genetic Algorithm Model. *Electronics*, 2020, vol. 9, no. 7, art. no, 1143. doi: https://doi.org/10.3390/electronics9071143.

4. Abdollahi A., Ghadimi A., Miveh M., Mohammadi F., Jurado F. Optimal Power Flow Incorporating FACTS Devices and Stochastic Wind Power Generation Using Krill Herd Algorithm. *Electronics*, 2020, vol. 9, no. 6, art. no. 1043. doi: https://doi.org/10.3390/electronics9061043.

5. *Global Wind Energy Council. Global Wind Report 2023*. 120 p. Available at: https://www.gwec.net/reports/globalwindreport/2023 (accessed on 27 March 2023).

6. *Global Wind Energy Council. Global Wind Report 2022*. 158 p. Available at: https://www.gwec.net/reports/globalwindreport/2022 (accessed on 27 March 2022).

7. Mlecnik E., Parker J., Ma Z., Corchero C., Knotzer A., Pernetti R. Policy challenges for the development of energy flexibility services. *Energy Policy*, 2020, vol. 137, art. no. 111147. doi: https://doi.org/10.1016/j.enpol.2019.111147.

8. Lu Y., Khan Z.A., Alvarez–Alvarado M.S., Zhang Y., Huang Z., Imran M. A Critical Review of Sustainable Energy Policies for the Promotion of Renewable Energy Sources. *Sustainability*, 2020, vol. 12, no. 12, art. no. 5078. doi: https://doi.org/10.3390/su12125078.

9. Schwarz M., Nakhle C., Knoeri C. Innovative designs of building energy codes for building decarbonization and their implementation challenges. *Journal of Cleaner Production*, 2020, vol. 248, art. no. 119260. doi: https://doi.org/10.1016/j.jclepro.2019.119260.

10. Nazir M.S., Mahdi A.J., Bilal M., Sohail H.M., Ali N., Iqbal H.M.N. Environmental impact and pollution–related challenges of renewable wind energy paradigm – A review. *Science of The Total Environment*, 2019, vol. 683, pp. 436–444. doi: https://doi.org/10.1016/j.scitotenv.2019.05.274.

11. Andrić I., Koc M., Al–Ghamdi S.G. A review of climate change implications for built environment: Impacts, mitigation measures and associated challenges in developed and developing countries. *Journal of Cleaner Production*, 2019, vol. 211, pp. 83–102. doi: https://doi.org/10.1016/j.jclepro.2018.11.128.

12. Bourouina A., Taleb R., Bachir G., Boudjema Z., Bessaad T., Saidi H. Comparative analysis between classical and third–order sliding mode controllers for maximum power extraction in wind turbine system. *Electrical Engineering & Electromechanics*, 2025, no. 3, pp. 18–22. doi: https://doi.org/10.20998/2074–272X.2025.3.03.

13. Belayneh B.A., Tuka M.B. Performance analysis of doubly fed induction generator in wind energy conversion system by controlling active and reactive power. *Research Square*, 2022. pp. 1–14. doi: https://doi.org/10.21203/rs.3.rs–2152568/v1.

14. Son J.–Y., Ma K. Wind Energy Systems. *Proceedings of the IEEE*, 2017, vol. 105, no. 11, pp. 2116–2131. doi: https://doi.org/10.1109/JPROC.2017.2695485.

15. Yang B., Jiang L., Wang L., Yao W., Wu Q.H. Nonlinear maximum power point tracking control and modal analysis of DFIG based wind turbine. *International Journal of Electrical Power & Energy Systems*, 2016, vol. 74, pp. 429–436. doi: https://doi.org/10.1016/j.ijepes.2015.07.036.

16. Holttinen H., Hirvonen R. Power System Requirements for Wind Power. *Wind Power in Power Systems*, 2005, pp. 143–167. doi: https://doi.org/10.1002/0470012684.ch8.

17. Kazachkov Y.A., Feltes J.W., Zavadil R. Modeling wind farms for power system stability studies. *2003 IEEE Power Engineering Society General Meeting*, 2003, pp. 1526–1533. doi: https://doi.org/10.1109/PES.2003.1267382.

18. Rodriguez J.M., Fernandez J.L., Beato D., Iturbe R., Usaola J., Ledesma P., Wilhelmi J.R. Incidence on power system dynamics of high penetration of fixed speed and doubly fed wind energy systems: study of the Spanish case. *IEEE Transactions on Power Systems*, 2002, vol. 17, no. 4, pp. 1089–1095. doi: https://doi.org/10.1109/TPWRS.2002.804971.

19. Beainy A., Maatouk C., Moubayed N., Kaddah F. Comparison of different types of generator for wind energy conversion system topologies. *2016 3rd International Conference on Renewable Energies for Developing Countries (REDEC)*, 2016, pp. 1–6. doi: https://doi.org/10.1109/REDEC.2016.7577535.

20. Reddy S.S., Prathipati K., Lho Y.H. Transient Stability Improvement of a System Connected with Wind Energy Generators. *International Journal of Emerging Electric Power Systems*, 2017, vol. 18, no. 5, pp. 20170063. doi: https://doi.org/10.1515/ijeeps–2017–0063.

21. Maity D., Chowdhury A., Reddy S.S., Panigrahi B.K., Abhyankar A.R., Mallick M.K. Joint energy and spinning reserve dispatch in wind–thermal power system using IDE–SAR technique. *2013 IEEE Symposium on Swarm Intelligence (SIS)*, 2013, pp. 284–290. doi: https://doi.org/10.1109/SIS.2013.6615191.

22. Yi Zhang, Ula S. Comparison and evaluation of three main types of wind turbines. *2008 IEEE/PES Transmission and Distribution Conference and Exposition*, 2008, pp. 1–6. doi: https://doi.org/10.1109/TDC.2008.4517282.

23. Abdel–Khalik A.S., Ahmed K.H. Performance evaluation of grid connected wind energy conversion systems with five–phase modular permanent magnet synchronous generators having different slot and pole number combinations. *2011 IEEE International Electric Machines & Drives Conference (IEMDC)*, 2011, pp. 1119–1124. doi: https://doi.org/10.1109/IEMDC.2011.5994758.

24. Chowdhury M.M., Haque M.E., Aktarujjaman M., Negnevitsky M., Gargoom A. Grid integration impacts and energy storage systems for wind energy applications – A review. *2011 IEEE Power and Energy Society General Meeting*, 2011, pp. 1–8. doi: https://doi.org/10.1109/PES.2011.6039798.

25. Duan J.D., Li R., An L. Study of Voltage Stability in Grid–Connected Large Wind Farms. *Advanced Materials Research*, 2012, vol. 433–440, pp. 1794–1801. doi: https://doi.org/10.4028/www.scientific.net/AMR.433–440.1794.

26. Behabtu H.A., Coosemans T., Berecibar M., Fante K.A., Kebede A.A., Mierlo J.V., Messagie M. Performance Evaluation of Grid–

Connected Wind Turbine Generators. *Energies*, 2021, vol. 14, no. 20, art. no. 6807. doi: https://doi.org/10.3390/en14206807.
27. Nid A., Sayah S., Zebar A. Power fluctuation suppression for grid connected permanent magnet synchronous generator type wind power generation system. *Electrical Engineering & Electromechanics*, 2024, no. 5, pp. 70–76. doi: https://doi.org/10.20998/2074–272X.2024.5.10.
28. Zine H.K.E., Abed K. Smart current control of the wind energy conversion system based permanent magnet synchronous generator using predictive and hysteresis model. *Electrical Engineering & Electromechanics*, 2024, no. 2, pp. 40–47. doi: https://doi.org/10.20998/2074–272X.2024.2.06.
29. Manikandan K., Sasikumar S., Arulraj R. A novelty approach to solve an economic dispatch problem for a renewable integrated micro–grid using optimization techniques. *Electrical Engineering & Electromechanics*, 2023, no. 4, pp. 83–89. doi: https://doi.org/10.20998/2074–272X.2023.4.12.
30. Oualah O., Kerdoun D., Boumassata A. Super–twisting sliding mode control for brushless doubly fed reluctance generator based on wind energy conversion system. *Electrical Engineering & Electromechanics*, 2023, no. 2, pp. 86–92. doi: https://doi.org/10.20998/2074–272X.2023.2.13.
31. Ekanayake J.B., Holdsworth L., XueGuang Wu, Jenkins N. Dynamic modeling of doubly fed induction generator wind turbines. *IEEE Transactions on Power Systems*, 2003, vol. 18, no. 2, pp. 803–809. doi: https://doi.org/10.1109/TPWRS.2003.811178.
32. Hannan M.A., Al–Shetwi A.Q., Mollik M.S., Ker P.J., Mannan M., Mansor M., Al–Masri H.M.K., Mahlia T.M.I. Wind Energy Conversions, Controls, and Applications: A Review for Sustainable Technologies and Directions. *Sustainability*, 2023, vol. 15, no. 5, art. no. 3986. doi: https://doi.org/10.3390/su15053986.
33. Saoudi Y., Abdallah H.H. Contribution of FACTS Device for Persisting Optimal Grid Performance Despite Wind Farm Integration. *International Review on Modelling and Simulations*, 2015, vol. 8, no. 2, pp. 147–153. doi: https://doi.org/10.15866/iremos.v8i2.3033.
34. Hajer H., Yahia S., Anouar B., Larbi C.–A., Taouali O. The Dynamic of the Grid with the Presence of WF and the AVR for Power Quality Enhancement. *2025 4th International Conference on Computing and Information Technology (ICCIT)*, 2025, pp. 629–632. doi: https://doi.org/10.1109/ICCIT63348.2025.10989368.
35. Milykh V.I. Numerical–field analysis of active and reactive winding parameters and mechanical characteristics of a squirrel–cage induction motor. *Electrical Engineering & Electromechanics*, 2023, no. 4, pp. 3–13. doi: https://doi.org/10.20998/2074–272X.2023.4.01.
36. Ramos T., Medeiros Júnior M.F., Pinheiro R., Medeiros A. Slip Control of a Squirrel Cage Induction Generator Driven by an Electromagnetic Frequency Regulator to Achieve the Maximum Power Point Tracking. *Energies*, 2019, vol. 12, no. 11, art. no. 2100. doi: https://doi.org/10.3390/en12112100.
37. García H., Segundo J., Rodríguez–Hernández O., Campos–Amezcua R., Jaramillo O. Harmonic Modelling of the Wind Turbine Induction Generator for Dynamic Analysis of Power Quality. *Energies*, 2018, vol. 11, no. 1, art. no. 104. doi: https://doi.org/10.3390/en11010104.
38. Patil N.S., Bhosle Y.N. A review on wind turbine generator topologies. *2013 International Conference on Power, Energy and Control (ICPEC)*, 2013, pp. 625–629. doi: https://doi.org/10.1109/ICPEC.2013.6527733.
39. Osman S.H.E., Irungu G.K., Murage D.K. Impact of Different Locations of Integrating SCIG Wind Turbine into Distributed Network Using Continuation Power Flow Method. *2019 International Conference on Computer, Control, Electrical, and Electronics Engineering (ICCCEEE)*, 2019, pp. 01–05. doi: https://doi.org/10.1109/ICCCEEE46830.2019.9071040.
40. Anusri P., Sindhu K.C. Mathematical Modeling of the Squirrel Cage Induction Generator based Wind Farm for Sub–Synchronous Resonance Analysis. *Indian Journal of Science and Technology*, 2016, vol. 9, no. 38, pp. 1–7. doi: https://doi.org/10.17485/ijst/2016/v9i38/101943.
41. Hafaiedh H., Saoudi Y., Benamor A., Chrifi Alaoui L. Study of the impact of SCIG Wind farm integration and the effect of the location bus in dynamic grid enhancement. *2022 10th International Conference on Systems and Control (ICSC)*, 2022, pp. 114–118. doi: https://doi.org/10.1109/ICSC57768.2022.9993873.
42. Hannan M.A., Al–Shetwi A.Q., Mollik M.S., Ker P.J., Mannan M., Mansor M., Al–Masri H.M.K., Mahlia T.M.I. Wind Energy Conversions, Controls, and Applications: A Review for Sustainable Technologies and Directions. *Sustainability*, 2023, vol. 15, no. 5, art. no. 3986. doi: https://doi.org/10.3390/su15053986.
43. Yang W., Yang J. Advantage of variable–speed pumped storage plants for mitigating wind power variations: Integrated modelling and performance assessment. *Applied Energy*, 2019, vol. 237, pp. 720–732. doi: https://doi.org/10.1016/j.apenergy.2018.12.090.
44. El Amine B.B.M., Ahmed A., Houari M.B., Mouloud D. Modeling, simulation and control of a doubly–fed induction generator for wind energy conversion systems. *International Journal of Power Electronics and Drive Systems*, 2020, vol. 11, no. 3, pp. 1197–1210. doi: https://doi.org/10.11591/ijpeds.v11.i3.pp1197–1210.
45. Pandikumar M. A Control Methodology of Doubly Fed Induction Generator for Wind Energy Generation. *IOP Conference Series: Materials Science and Engineering*, 2020, vol. 937, no. 1, art. no. 012056. doi: https://doi.org/10.1088/1757–899X/937/1/012056.
46. Saoudi Y., Abdallah H.H. The effect of the injected active and reactive powers for the improvement of voltage amplitude and frequency qualities. *14th International Conference on Sciences and Techniques of Automatic Control & Computer Engineering – STA'2013*, 2013, pp. 47–51. doi: https://doi.org/10.1109/STA.2013.6783104.
47. Boukadoum A., Bouguerne A., Bahi T. Direct power control using space vector modulation strategy control for wind energy conversion system using three–phase matrix converter. *Electrical Engineering & Electromechanics*, 2023, no. 3, pp. 40–46. doi: https://doi.org/10.20998/2074–272X.2023.3.06.
48. Hatziargyriou N., Milanovic J., Rahmann C., Ajjarapu V., Canizares C., Erlich I., Hill D., Hiskens I., Kamwa I., Pal B., Pourbeik P., Sanchez–Gasca J., Stankovic A., Van Cutsem T., Vittal V., Vournas C. Definition and Classification of Power System Stability – Revisited & Extended. *IEEE Transactions on Power Systems*, 2021, vol. 36, no. 4, pp. 3271–3281. doi: https://doi.org/10.1109/TPWRS.2020.3041774.
49. Chi Y., Liu Y., Wang W., Dai H. Voltage Stability Analysis of Wind Farm Integration into Transmission Network. *2006 International Conference on Power System Technology*, 2006, pp. 1–7. doi: https://doi.org/10.1109/ICPST.2006.321661.
50. Sauer P.W., Pai M.A., Chow J.H. Power System Toolbox. *Power System Dynamics and Stability: With Synchrophasor Measurement and Power System Toolbox 2nd edition*, 2017, pp. 305–325. doi: https://doi.org/10.1002/9781119355755.ch11.
51. Kumar S., Kumar A., Sharma N.K. A novel method to investigate voltage stability of IEEE–14 bus wind integrated system using PSAT. *Frontiers in Energy*, 2020, vol. 14, no. 2, pp. 410–418. doi: https://doi.org/10.1007/s11708–016–0440–8.

Received 28.02.2025
Accepted 25.04.2025
Published 02.09.2025

H. Hafaiedh[1]*, PhD,*
Y. Saoudi[2]*, Doctor of Electrical Engineering,*
A. Benamor[3]*, Associate Professor,*
L. Chrifi–Alaoui[4]*, Associate Professor,*
[1] Higher National School of Engineering of Tunis,
University of Tunis, Tunisia,
e–mail: hajer.hafayedh@gmail.com (Corresponding Author)
[2] Laboratory of Control and Energy Management Laboratory,
National School of Engineering of Sfax, Tunisia.
[3] National School of Engineers of Monastir,
Laboratory of Automatic Signal and Image Processing,
University of Monastir, Tunisia.
[4] Laboratory of Innovative Technologies,
University of Picardy Jules Verne, France.

How to cite this article:
Hafaiedh H., Saoudi Y., Benamor A., Chrifi–Alaoui L. Wind farms integration into power system with improved location and stability problem solving. *Electrical Engineering & Electromechanics*, 2025, no. 5, pp. 10-16. doi: https://doi.org/10.20998/2074-272X.2025.5.02